



## 25 **Abstract**

26 To increase the throughput, lower the cost, and save scarce test reagents,  
27 laboratories can pool patient samples before SARS-CoV-2 RT-qPCR testing. While  
28 different sample pooling methods have been proposed and effectively implemented  
29 in some laboratories, no systematic and large-scale evaluations exist using real-life  
30 quantitative data gathered throughout the different epidemiological stages. Here, we  
31 use anonymous data from 9673 positive cases to simulate and compare 1D and 2D  
32 pooling strategies. We show that the optimal choice of pooling method and pool size  
33 is an intricate decision with a testing population-dependent efficiency-sensitivity  
34 trade-off and present an online tool to provide the reader with custom real-time  
35 pooling strategy recommendations.

36

37

## 38 Introduction

39 One of the key strategies in the global battle against the COVID-19 pandemic is  
40 massive population testing. However, an ongoing shortage of time, reagents and  
41 testing capacity has tempered these efforts. Pooled testing of samples presents itself  
42 as a valid strategy to overcome these hurdles and to realize rapid, large-scale testing  
43 at lower cost and lower dependence on test reagents.

44

45 Multiple recent studies discussed pooling strategies in the frame of SARS-CoV-2  
46 testing. Researchers have explored many strategies, but two of them have been  
47 welcomed for their simplicity and effectiveness: one-time pooling (1D pooling) and  
48 two-dimensional pooling (2D pooling). In 1D pooling, the samples are pooled, pools  
49 are tested and samples in positive pools are tested individually (Figure 1)<sup>1-4</sup>. Labs  
50 worldwide have extensively evaluated 1D pooling strategies for SARS-CoV-2 testing  
51 in the lab<sup>5-8</sup> or using simulations<sup>1</sup>. In 2D pooling, samples are organized in a 2D  
52 matrix and pools are created along the matrix's rows and columns. The pools are  
53 tested, and negative rows and columns are excluded from the matrix. Next, all  
54 remaining samples are tested individually (Figure 1)<sup>9</sup>. Other more complex strategies  
55 exist, such as repeated pooling<sup>1</sup>, P-BEST<sup>10</sup> and Tapestry<sup>11</sup>.

56

57 While attractive, pooling strategies come with inherent limitations. First, pooling  
58 dilutes each sample, possibly to such an extent that the viral RNA becomes  
59 undetectable, which results in false negative observations<sup>8,9,12</sup>. A second limitation is  
60 that an increase in sample manipulations augments the risk of cross-contamination  
61 and sample mix-ups, possibly leading to false negatives and false positives<sup>9</sup>. Last,  
62 when pooling, identifying individual positive samples will take an additional RNA

63 extraction and RT-qPCR run, while one run is sufficient when testing individual  
64 samples without pooling, which increases labor and turnaround time.

65

66 Although the number of preprints and peer-reviewed publications on pooling  
67 strategies for COVID-19 RT-qPCR-based testing has accelerated rapidly throughout  
68 the pandemic, some critical aspects remain mostly ignored. First of all, the proposed  
69 optimal pooling strategy is most often based on a binary classification of samples as  
70 either positive or negative. This Boolean approach is not true to the real-world  
71 situation and does not investigate the pooling step's dilution effect. Second, when  
72 using Cq values as a semi-quantitative measure<sup>13</sup> of the viral loads, their overall  
73 distribution should reflect the real-life population. A high fraction of Cq values close to  
74 the limit of detection of the RT-qPCR assay produces an elevated risk of resulting in  
75 false negative samples<sup>14</sup>. Last, since the Cq distribution of the sample population and  
76 prevalence may vary over time, it remains unclear how the pooling strategy's  
77 performance evolves as the pandemic progresses.

78

79 We questioned to what extent optimal pooling strategies would have changed  
80 throughout the COVID-19 pandemic and how testing facilities might use pooling  
81 strategies for future testing in a correct and attainable manner. To this extent, we  
82 simulated and evaluated one-dimensional (1D) and two-dimensional (2D) pooling  
83 strategies with different pool sizes using real-life RT-qPCR data gathered by the  
84 Belgian national testing platform during the end of the first and the beginning of the  
85 second SARS-CoV-2 epidemiological waves. Additionally, we formulate a detailed  
86 action plan to provide testing laboratories with the most suitable pooling strategy  
87 assuring an optimal efficiency-sensitivity trade-off.

88

## 89 **Materials and Methods**

### 90 *Patient samples*

91 Nasopharyngeal swabs were collected in VTM or DNA/RNA Shield (Zymo Research)  
92 by a healthcare professional as a diagnostic test for SARS-CoV-2, as part of the  
93 Belgian national testing platform. The individuals were tested at nursing homes or in  
94 triage centers, between April 9<sup>th</sup> and June 7<sup>th</sup>, and between September 1<sup>st</sup> and  
95 November 10<sup>th</sup>. After filtering the data as described further, this resulted in 207 944  
96 patients in total, of which 9673 positives (4.65%).

97

### 98 *SARS-CoV-2 RT-qPCR test*

99 During the first (spring) wave, RNA extraction was performed using the Total RNA  
100 Purification Kit (Norgen Biotek #24300) according to the manufacturer's instructions  
101 using 200 µl transport medium, 200 µl lysis buffer and 200 µl ethanol, with  
102 processing using a centrifuge (5810R with rotor A-4-81, both from Eppendorf). RNA  
103 was eluted from the plates using 50 µl elution buffer (nuclease-free water), resulting  
104 in approximately 45 µl eluate. RNA extractions were simultaneously performed for 94  
105 patient samples and 2 negative controls (nuclease-free water). After addition of the  
106 lysis buffer, 4 µl of a proprietary 700 nucleotides spike-in control RNA (prior to May  
107 25<sup>th</sup>, 40 000 copies for singleplex RT-qPCR; from May 25<sup>th</sup> onwards, 5000 copies for  
108 duplex RT-qPCR) and carrier RNA (200 ng of yeast tRNA, Roche #10109517001)  
109 was added to all 96 wells from the plate. To the eluate of one of the negative control  
110 wells, 7500 RNA copies of positive control RNA (Synthetic SARS-CoV-2 RNA  
111 Control 2, Twist Biosciences #102024) were added. During the second (autumn)  
112 wave, RNA extraction was performed using the Quick-RNA Viral 96 Kit (Zymo

113 Research #R1041), according to the manufacturer's instructions using 100 µl  
114 transport medium, with processing using a centrifuge (5810R with rotor A-4-81, both  
115 from Eppendorf). RNA was eluted from the plates using 30 µl elution buffer  
116 (nuclease-free water). RNA extractions were simultaneously performed for 92 patient  
117 samples, 2 negative controls (nuclease-free water), and 2 positive controls (1 diluted  
118 positive case as a full workflow control; 1 positive control RNA as RT-qPCR control,  
119 see further). After addition of the lysis buffer, 4 µl of a proprietary 700 nucleotides  
120 spike-in control RNA (5000 copies) and carrier RNA (200 ng of yeast tRNA, Roche  
121 #10109517001) was added to all 96 wells from the plate. To the eluate of one of the  
122 negative control wells, 7500 RNA copies of positive control RNA (Synthetic SARS-  
123 CoV-2 RNA Control 2, Twist Biosciences #102024) were added.

124 Six µl of RNA eluate was used as input for a 20 µl RT-qPCR reaction in a CFX384  
125 qPCR instrument using 10 µl iTaq one-step RT-qPCR mastermix (Bio-Rad  
126 #1725141) according to the manufacturer's instructions, using 250 nM final  
127 concentration of primers and 400 nM of hydrolysis probe. Primers and probes were  
128 synthesized by Integrated DNA Technologies using clean-room GMP production. For  
129 detection of the SARS-CoV-2 virus, the Charité E gene assay was used (FAM)<sup>15</sup>; for  
130 the internal control, a proprietary hydrolysis probe assay (HEX) was used. Prior to  
131 May 25<sup>th</sup>, 2 singleplex assays were performed; from May 25<sup>th</sup> onwards, 1 duplex RT-  
132 qPCR was performed. Cq values were generated using the FastFinder software  
133 v3.300.5 (UgenTec). Only batches were approved with a clean negative control and  
134 a positive control in the expected range.

135

136 *Digital PCR calibration of positive control RNA*

137 Digital PCR was done on a QX200 instrument (Bio-Rad) using the One-Step RT-  
138 ddPCR Advanced Kit for Probes (Bio-Rad #1864022) according to the  
139 manufacturer's instructions. Briefly, 22  $\mu$ l pre-reactions were prepared consisting of 5  
140  $\mu$ l 4x supermix, 2  $\mu$ l reverse transcriptase, 6  $\mu$ l positive control RNA (125 RNA  
141 copies/ $\mu$ l), 15 mM dithiothreitol, 900 nM of each forward and reverse primer and 250  
142 nM *E* gene hydrolysis probe (FAM) (see higher). 20  $\mu$ l of the pre-reaction was used  
143 for droplet generation using the QX200 Droplet Generator, followed by careful  
144 transfer to a 96-well PCR plate for thermocycling: 60 min 46 °C reverse transcription,  
145 10 min 95 °C enzyme activation, 40 cycles of 30 sec denaturation at 95 °C and 1 min  
146 annealing/extension at 59 °C, and finally 10 min 98 °C enzyme deactivation. Droplets  
147 were analyzed by the QX200 Droplet Reader and QuantaSoft software. With an RNA  
148 input of 7500 copies per reaction, the digital PCR result was 1500 cDNA copies (or  
149 20% of the expected number, a fraction confirmed by Dr. Jim Huggett for particular  
150 lot numbers of #102024, personal communication. The reason for this discrepancy is  
151 two-fold: the number of RNA molecules provided by the manufacturer is only  
152 approximate, and the reverse transcription reaction is inefficient). The median Cq  
153 value of the positive control RNA of 24.55 thus corresponds to 1500 digital PCR  
154 calibrated cDNA molecules.

155

156 *Determination of efficiency and sensitivity for simulated of 1D and 2D pooling*  
157 *strategies*

158 Simulations are run using R 4.0.1. First, several cohorts of 100 000 patients are  
159 repeatedly simulated with varying fractions of positive cases  $f$ , depending on the  
160 fraction of positive samples of the investigated week. This is done five times,  
161 resulting in five replicate cohorts per week. The Cq values of the positive samples

162 are sampled with replacement from the set of the positive Cq values of said week.  
163 Next, the patients are randomly separated into pools depending on the pooling  
164 strategy that is simulated. The pooling strategies that were simulated are 1x4, 1x8,  
165 1x12, 1x16, 1x24 (all 1D), and 8x12, 12x16 and 16x24. The Cq value of the pool was  
166 calculated as follows:  
167

$$c_{pool} = \log_2 P - \log_2 \sum_{i=1}^p 2^{-c_i} \quad \#(1)$$

168  
169  
170 With  $c_{pool}$  the Cq value of the pool,  $P$  the number of samples in the pool,  $p$  the  
171 number of positive samples in the pool,  $c_1, c_2, \dots, c_p$  the Cq values of the positive  
172 samples. If the Cq value of the pool is lower than the single-molecule Cq value, it is  
173 classified as a positive pool. For 1D pooling, only samples in positive pools are  
174 retained and the remaining individual Cq values were checked to be positive. For 2D  
175 pooling, the Cq values of the differently sized pools are checked simultaneously and  
176 the samples in negative pools are removed, after which all Cq values of the  
177 remaining samples are checked individually. Samples that were retained after the  
178 testing of the pools and that had an individual Cq lower than the single-molecule Cq  
179 value are classified as positive, all other samples are classified as negative.

180 The sensitivity is calculated as:

181

$$sensitivity = \frac{no. \ true \ positive \ samples}{no. \ true \ positive \ samples + no. \ false \ negative \ samples} \quad \#(2)$$

182

183



184 The analytical efficiency gain is calculated as:

185

$$efficiency\ gain = \frac{no.\ tests\ required\ for\ individual\ testing}{no.\ tests\ required\ for\ pooling\ strategy} \#(3)$$

186

187

188 In all simulations, the number of tests required for individual testing is equal to the  
189 number of samples (assuming no technical failures). The outcomes for each  
190 simulation were identical as the sample size far outreached the size of the dataset.

191 The code is available at <https://github.com/OncoRNALab/covidpooling>.

192

193 *Ad hoc sensitivity and efficiency calculation*

194 To calculate the efficiency for a specific 1D pooling strategy on a real sample set, the  
195 following equation was used:

$$efficiency = \frac{n}{\frac{n}{s} \cdot (1 + s \cdot \sum_{k=1}^s \left( \frac{s!}{k!(s-k)!} \cdot p^k \cdot (1-p)^{s-k} \cdot (1-c^k) \right))} \#(4)$$

196

197 With sample size  $n$ , pool size  $s$ , fraction of positive samples  $p$  and fraction of Cq  
198 values of positive samples above the 'dilution detection limit': the lowest individual Cq  
199 value that can result in a pooled Cq value lower than the single molecule Cq value,  
200 or:

$$single\ molecule\ Cq\ value - \log_2(pool\ size) \#(5)$$

201

202 Equation (4) is derived as follows. The efficiency is defined by the following equation:

$$efficiency = \frac{n}{no.\ tests\ required\ for\ pooling\ strategy} \#(6)$$

203

204 The number of tests performed when using a pooling strategy is equal to:

$$\text{no. tests required for pooling strategy} = \text{no. pools} + \text{no. positive pools} \cdot s \#(7)$$

205

206 Since  $\# \text{ pools} = \frac{n}{s}$ ,

$$\text{no. tests required for pooling strategy} = \frac{n}{s} + \text{no. positive pools} \cdot s \#(8)$$

207 The exact number of positive pools can be calculated by multiplying the number of  
208 pools by the probability of a pool testing positive. Approximately, a pool will test  
209 positive if it includes a positive sample with a Cq value lower than the 'dilution  
210 detection limit'. The probability of having a specific number of positive samples  $k$  in a  
211 pool with pool size  $s$  is defined by a binomial distribution:

$$\frac{s!}{k!(s-k)!} \cdot p^k \cdot (1-p)^{s-k} \#(8)$$

212

213 Thus, the probability of having at least one positive value in a pool is equal to:

$$\sum_{k=1}^s \left( \frac{s!}{k!(s-k)!} \cdot p^k \cdot (1-p)^{s-k} \right) \#(10)$$

214

215 In general, we can assume that when a sample has a Cq value higher than the  
216 'dilution detection limit', for the sample to test positive, it must be accompanied by a  
217 sample with a Cq value lower than the 'dilution detection limit'. Equation (10) can be  
218 adjusted to factor for these events:

$$\sum_{k=1}^s \left( \frac{s!}{k!(s-k)!} \cdot p^k \cdot (1-p)^{s-k} \cdot (1-c^k) \right) \#(10)$$

219

220 Filling in Eq. (10) in Eq. (8) results in the final formula being used for the calculation  
221 of the efficiency.

222

223 To estimate the sensitivity for a specific 1D pooling strategy on a real sample set, the  
224 following equation was used:

$$sensitivity = c \cdot \sum_{k=0}^{s-1} \left( \frac{(s-1)!}{k! ((s-1)-k)!} \cdot p^k \cdot (1-p)^{(s-1)-k} \cdot (1-c^k) \right) + (1-c) \quad \#(11)$$

225

226 The sensitivity can be defined as the probability a true positive sample tests positive.

227 For our situation it will be equal to the probability that any sample tests positive:

$$P(pos\ test) = P(pos\ test|Cq \geq\ cut\ off) \cdot P(Cq \geq\ cut\ off) + \\ P(pos\ test|Cq <\ cut\ off) \cdot P(Cq <\ cut\ off) \quad \#(12)$$

228

229 Previously,  $P(Cq \geq\ cut\ off)$  was defined as  $c$  and therefore  $P(Cq <\ cut\ off) = 1 - c$ .

230 Also  $P(pos\ test|Cq <\ cut\ off) = 1$ . A positive sample with Cq value above the

231 'dilution detection limit' can only test positive if one of the other samples in the pool is

232 also positive and has a Cq value lower than the 'dilution detection limit'. We can

233 calculate the probability of this happening by using the same logic as before, but with

234  $s - 1$  instead of  $s$ :

$$\sum_{k=0}^{s-1} \left( \frac{(s-1)!}{k! ((s-1)-k)!} \cdot p^k \cdot (1-p)^{(s-1)-k} \cdot (1-c^k) \right) \quad \#(13)$$

235

236 Completing Eq. (12) with Eq. (13) leads to Eq. (11) for calculating the sensitivity.

237

238 *Web application*

239 To help laboratories find the best pooling strategy for their specific situation (i.e. the  
240 local positivity ratio and Cq value distribution), we developed a Shiny application in R  
241 4.0.1. The Shiny application was launched on our in-house Shiny server and is  
242 available at <https://shiny.dev.cmgg.be/>.

243

244

## 245 **Results**

### 246 *Single-molecule Cq value determination*

247 We made a 5-point 10-fold serial dilution series of positive control RNA from 150 000  
248 (digital PCR calibrated) copies down to 15 copies. The Y-intercept value points at a  
249 single-molecule Cq value of 35.66 and 35.28 for singleplex and duplex RT-qPCR,  
250 respectively (Supplemental Figure 1). Therefore, we conservatively use 37 as the  
251 single-molecule value for further analysis. Patient sample Cq values higher than the  
252 single-molecule Cq value threshold are likely due to random measurement variation,  
253 lot reagent variability and sample inhibition.

254

### 255 *Cq distribution is dynamic over course of the pandemic*

256 Few studies have explored how the Cq value distribution within one testing facility  
257 evolves during the COVID-19 pandemic. We determined the 75%-tile of the Cq value  
258 distribution and the percentage of positive tests per day as a proxy for actual Cq  
259 value distribution and prevalence, respectively (Figure 2). We compared the fraction  
260 of positive tests in our dataset with the fraction of positive tests as reported by the  
261 federal agency for public health Sciensano (<https://epistat.wiv-isp.be/covid/>  
262 accessed January 25<sup>th</sup>, 2021). First, the fractions of positive tests seem to align at  
263 the end of the first wave, but in the second wave our data seems to be shifted about

264 one to two weeks later. Second, the 75%-tile of the Cq values varies over the course  
265 of the pandemic from a minimum value of around 18 and a maximum value of almost  
266 35. Third, when comparing the fraction of positive samples and the 75%-tile of the Cq  
267 value distribution, we note that these parameters are inversely related: when the  
268 positivity rate goes down, the Cq value distribution shifts towards the higher end of  
269 the spectrum (Supplemental Figure 2). In conclusion, the Cq value distribution and  
270 prevalence show a dynamic profile over the course of the COVID-19 pandemic.  
271 These observations are crucial considering that positivity rate and Cq value  
272 distribution are key determinants of efficiency and sensitivity of any pooling strategy.

273

#### 274 *Pooling efficiency and sensitivity changes as pandemic progresses*

275 To explore how hypothetical pooling strategies would have affected the SARS-CoV-2  
276 testing outcomes, we simulated different 1D (with pool size of 4, 8, 12, 16 and 24)  
277 and 2D pooling (with pool sizes of 8x12, 12x16, and 16x24) strategies using  
278 individual sample Cq values from a single Belgian laboratory during the end of the  
279 first and beginning of the second wave. The data was grouped by week and the  
280 resulting Cq value distributions and positivity rates were used as input for the  
281 simulations (Figure 3). First, sensitivity and efficiency show very opposing patterns  
282 when comparing different timeframes during the pandemic. At the end of the first  
283 wave the efficiency increases, while at the beginning of the second wave, the  
284 efficiency decreases. The sensitivity drops as we move further away from the first  
285 wave but remains stable as we enter the second. Second, pool size and strategy  
286 have a major influence on the outcomes. 2D pooling strategies generally have the  
287 highest efficiency, but the lowest sensitivity. Curiously, strategies with larger pool  
288 sizes were more efficient during the end of the first wave, but less efficient during the

289 beginning of the second wave. The sensitivity was always higher for strategies with  
290 smaller pool sizes, irrespective of the time during the pandemic. We conclude that—  
291 just like the positivity rate and the Cq value distribution—the sensitivity and efficiency  
292 depend on the timing in the pandemic and are heavily affected by the pooling  
293 strategy and the size of the pools.

294

#### 295 *Positivity rate drives efficiency, Cq distribution drives sensitivity*

296 We wondered how the positivity rate, Cq value distribution and pooling strategy affect  
297 the performance of the adopted strategy. To investigate this, we used the previous  
298 simulations for the end of the first wave to create an adjusted visualization where all  
299 parameters involved are incorporated (Figure 4). First, it is apparent that weeks with  
300 a high 75%-tile Cq value tend to have a low sensitivity and weeks with a high  
301 positivity rate seem to have a low efficiency. Second, pooling strategies with smaller  
302 pool sizes seem less sensitive to changes in positivity rate and Cq value distribution,  
303 as indicated by the area of the polygon traced around the edges of the data (Figure  
304 4). These results show that the prevalence mainly contributes to the efficiency and  
305 the Cq distribution to the sensitivity.

306

#### 307 *Shiny app for guided decision making*

308 To provide laboratories with a custom pooling strategy recommendation based on  
309 their specific sampling population, we worked out equations to estimate the  
310 sensitivity and efficiency (for 1D pooling strategies) based on an uploaded dataset of  
311 Cq values. The derivation of these equations can be found in the Methods section.  
312 We focused on 1D pooling strategies since 2D pooling strategies generally resulted  
313 in extreme outcomes (highest efficiency and lowest sensitivity) and the outcomes of

314 the optimal pooling strategy are situated somewhere in two extremes. To evaluate  
315 the equations' capacities to replicate the simulations, we compared the simulated  
316 efficiency and sensitivity of the pooling strategies for the different weeks and the  
317 efficiency and sensitivity of the pooling strategies the distributions, fraction of positive  
318 samples and single-molecule cutoff as inputs for the formulas (Supplemental Figure  
319 3 and Supplemental Figure 4). We integrated these formulas into an open-access  
320 Shiny application (Supplemental Figure 5). The application requires three inputs: a  
321 dataset of Cq values from positive samples, the positivity rate and the single-  
322 molecule cut-off Cq value. The Shiny application will then swiftly output the estimated  
323 data-specific efficiency and sensitivity for different pooling strategies.

324

## 325 **Discussion**

326 Using a sizeable real-life dataset of 9673 SARS-CoV-2 positive nasopharyngeal  
327 samples, we found that the pooling strategies' sensitivity and efficiency mainly  
328 depend on the prevalence and the distribution of the Cq values. Our results indicate  
329 that both the prevalence and the Cq value distribution are dynamic parameters  
330 during the SARS-CoV-2 pandemic and that, as a result, the resulting sensitivity and  
331 efficiency of pooling strategies are as well. To enable researchers and institutions  
332 with a real-time and accessible recommendation concerning the optimal 1D pooling  
333 strategy for their testing population, we developed a Shiny app providing just that.

334 Two factors could explain the dynamics of the prevalence and the Cq value  
335 distribution: epidemiological and virological change within the same sampling  
336 population and variation in the sampling population. The existence of these factors  
337 would suggest that an intricate interplay of these two components is at the origin of  
338 the observed evolutions. Recent research indicated that the first component

339 (epidemiological change) exists, as the distribution of random surveillance testing-  
340 deduced Cq values fluctuates during the SARS-CoV-2 pandemic (by definition, no  
341 changes in sampling population occurred in this research, thereby excluding this  
342 factor from the equation)<sup>16</sup>. As such, an alarming change in reproduction number  
343 (inherently coupled to the epidemiological period) should induce a reassessment of  
344 the pooling strategy<sup>17</sup>. The second component (variation in sampling population) is  
345 bound to happen when the testing facility is not consistently receiving samples from  
346 the same origin, as is the case for Biogazelle. At the very introduction of Biogazelle  
347 as a testing facility, most samples originated from hospitals and sources were added  
348 progressively as the testing capacity increased. Additionally, the Belgian government  
349 instituted a rapid change in the testing regime on October 21<sup>st</sup>, 2020: only  
350 symptomatic suspected SARS-CoV-2 cases get tested. The federal government lifted  
351 this measure on November 23<sup>rd</sup>, 2020, when the number of cases lowered and the  
352 existing testing capacity sufficed again. Since symptomatic patients generally show  
353 lower Cq values<sup>18,19</sup>, it is clear that sampling bias will contribute to the overall Cq  
354 value distribution.

355 The influence these dynamic parameters have on the variation of performance of  
356 pooling strategies is significant. This observation raises an issue for interpreting  
357 pooling strategy evaluations not based on time-series datasets. The effectiveness of  
358 a chosen pooling plan might even decrease to such an extent that it becomes inferior  
359 to individual testing. We observed this situation at the end of the second wave when  
360 efficiency is close to 1, but sensitivity is not (Figure 3). Based on these results, it  
361 becomes essential to regularly re-evaluate an adopted pooling strategy to avoid  
362 compromising on sensitivity and efficiency when there is no need.



363 Multiple effects contribute to how the testing population's characteristics drive pooling  
364 strategy outcomes. The main trends show that the prevalence mainly influences  
365 efficiency, and the Cq value distribution mainly influences sensitivity (Figure 3). We  
366 can explain both observations by using common sense and basic mathematics.  
367 When the prevalence is low, the efficiency is high: fewer pools will have positive  
368 samples and therefore test negative, which will automatically result in a lower number  
369 of tests needed to test all samples. Additionally, when a considerable proportion of  
370 samples have a Cq value close to the single-molecule Cq value, a more significant  
371 fraction of samples will become too diluted to detect during pooling and result in false  
372 negatives. There appear to be secondary compensating effects of the Cq value  
373 distribution and prevalence on the efficiency and sensitivity, respectively, which are  
374 more subtle. Primarily, as a higher fraction of positive samples has a Cq value close  
375 to the upper limit, more pools will test (false) negative, boosting the efficiency. On the  
376 other hand, when the prevalence increases, the sensitivity will increase due to an  
377 effect we call 'rescuing': a high Cq value that would otherwise test negative when  
378 diluted in the pool is 'rescued' by a low Cq value in the same pool. When the  
379 prevalence rises, the chances of this phenomenon happening also increase and as  
380 will the sensitivity. The same was observed by Cleary et al.<sup>17</sup>. Although minor, these  
381 secondary effects explain a number of our observations.

382 To elaborate how the optimal pooling strategy (best efficiency trade-off) transforms  
383 over time, assume two situations: low prevalence and high prevalence. When the  
384 prevalence is low, the larger pool sizes will result in higher efficiency and lower  
385 prevalence (more dilution). However, when the prevalence is high, the 'rescuing'  
386 effect will be more prominent and counteract the increasing efficiency and decreasing  
387 sensitivity. These results are in line with the widely accepted idea that sample pooling

388 methods show a higher efficiency when pool size is large and that as prevalence  
389 increases, it reached a threshold after which smaller pool sizes become more  
390 efficient<sup>1,9</sup>. Intuitively, the ‘rescuing’ effect is less prominent in 2D pooling strategies,  
391 as both pools (row and column) need to rescue the high Cq sample.  
392 False negatives have pre-pool Cq values close to the detection limit and  
393 predominantly originate from patients who are at the end of an infection<sup>17,20</sup>, putting  
394 their clinical relevance in question (i.e. no longer infectious). Similarly, however, one  
395 can argue that these high Cq samples are imperative to a favorable pandemic  
396 response: they might originate from pre-symptomatic or very recently-infected  
397 patients<sup>17</sup>, allowing for catching cases before transmission—a principle at the very  
398 core of every population screening strategy. Also, we cannot rule out that these high  
399 Cq values are due to imperfect sampling or any other mistakes along the sample  
400 preparation<sup>13</sup>.

401 Our study suffers from some essential limitations. First, although the data grouped by  
402 weeks provides many different situations to assess, there will still be other  
403 combinations of parameters that we did not analyze in this paper. However, the  
404 current dataset probably represents the most plausible scenarios as the data  
405 originates from a protracted period of the pandemic. Second, we selected only 1D  
406 and 2D pooling methods in this simulation study. As stated before, other pooling  
407 regimes exist and might be more performant than the discussed ones. Yet, these  
408 pooling strategies come with intrinsic shortcomings. The P-BEST pooling protocol is  
409 very time consuming<sup>10</sup>, even when using a pipetting robot, and the repeated pooling  
410 method suffers from a complicated re-pooling scheme<sup>1</sup>. Third, our model relies on  
411 the critical assumption that we can directly induce the pool’s Cq value from the  
412 individual samples’ Cq values using a simple formula (see Methods). Wet lab

413 experiments have shown that this is not necessarily the case<sup>5-8</sup>. Fourth, to calculate  
414 the pooling strategies' performance, the single-molecule Cq value and the  
415 prevalence must be known. However, we can easily calculate the single-molecule Cq  
416 value by generating a ddPCR calibrated dilution series as done in this paper. A  
417 testing laboratory can also choose to utilize a cut-off Cq value different from the  
418 single-molecule Cq value. Once a threshold Cq value is determined, it should not be  
419 changed. The prevalence, however, cannot be known precisely, and as a result, the  
420 prevalence must be estimated. We can do this either before adopting a pooling  
421 strategy by testing the individual samples and using the fraction of positive samples  
422 as an indication for the prevalence or when a pooling strategy is already in place by  
423 calculating it from the percentage of positive pools<sup>2,17</sup>. Last, the calculated efficiency  
424 gain is merely a representation of the number of individual RNA extractions and RT-  
425 qPCR reactions and does not evaluate the amount of labor or time-to-result. Pooling  
426 a low number of samples will unnecessarily increase the time-to-result and workload.  
427 In conclusion, we show that finding the optimal pooling strategy for SARS-CoV-2 test  
428 samples is guided by a testing population-dependent efficiency-sensitivity trade-off.  
429 Consequently, the most favorable pooling regime might change throughout the  
430 pandemic due to epidemiological changes and revisions in diagnostic testing  
431 strategies. We provide an accessible shiny application to guide readers towards the  
432 optimal pooling strategy to fit their needs.

433

## 434 **Acknowledgements**

435 We are grateful for the data from the Belgian federal taskforce for COVID-19 qPCR  
436 testing.

437

438 Conceptualization: J.Va., P.M. and J.Ve.; Methodology: J.Va., P.M. and J.Ve.;  
439 Software: J.Ve., T.S.; Formal Analysis: J.Ve.; Resources: J.H., J.Va. and P.M.; Data  
440 Curation: J.Ve.; Writing – Original Draft: J.Va. and J.Ve.; Writing – Review & Editing;  
441 J.Va., J.H., P.M., T.S. and J.Ve.; Visualisation: J.Va. and J.Ve.; Supervision: J.Va  
442 and P.M.; Project Administration: J.Va. and P.M.

443

#### 444 **Data availability**

445 The code and Cq values are available on  
446 <https://github.com/OncoRNALab/covidpooling>.

## 447 **References**

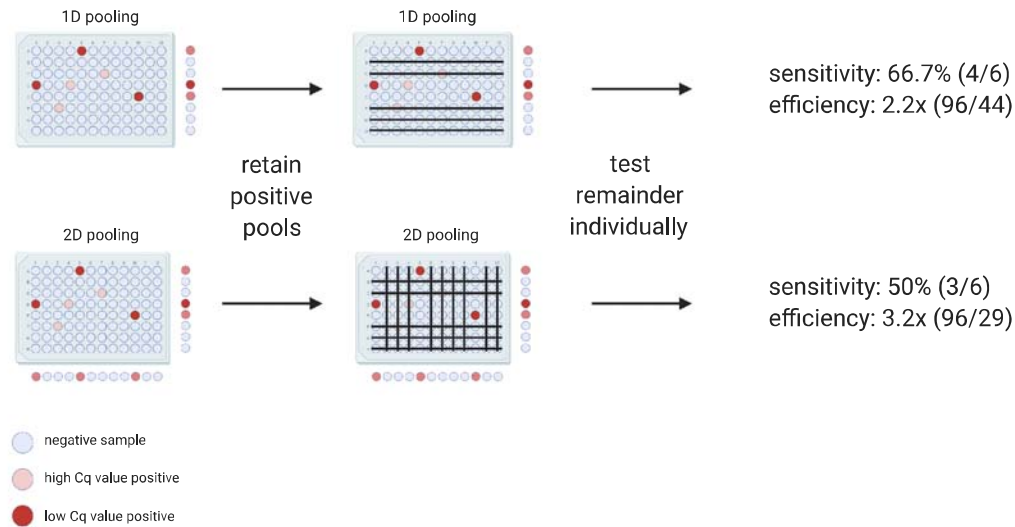
- 448 1. Shani-Narkiss, H., Gilday, O. D., Yayon, N. & Landau, I. D. Efficient and  
449 Practical Sample Pooling High-Throughput PCR Diagnosis of COVID-19.  
450 *medRxiv* 2020.04.06.20052159 (2020). doi:10.1101/2020.04.06.20052159
- 451 2. Guha, P., Guha, A. & Bandyopadhyay, T. Application of pooled testing in  
452 screening and estimating the prevalence of Covid-19. *medRxiv*  
453 2020.05.26.20113696 (2020). doi:10.1101/2020.05.26.20113696
- 454 3. Adams, K. Expanding Covid-19 Testing: Mathematical Guidelines for the  
455 Optimal Sample Pool Size Given Positive Test Rate. *medRxiv*  
456 2020.05.21.20108522 (2020). doi:10.1101/2020.05.21.20108522
- 457 4. Millionni, R. & Mortarino, C. Sequential informed pooling approach to detect  
458 SARS-CoV2 infection. *medRxiv* 2020.04.24.20077966 (2020).  
459 doi:10.1101/2020.04.24.20077966
- 460 5. Hogan, C. A., Sahoo, M. K. & Pinsky, B. A. Sample Pooling as a Strategy to  
461 Detect Community Transmission of SARS-CoV-2. *JAMA - Journal of the*  
462 *American Medical Association* **323**, 1967–1969 (2020).
- 463 6. Yelin, I. *et al.* Evaluation of COVID-19 RT-qPCR test in multi-sample pools.  
464 *Clin. Infect. Dis.* (2020). doi:<https://doi.org/10.1093/cid/ciaa531>
- 465 7. Abdalhamid, B. *et al.* Assessment of Specimen Pooling to Conserve SARS  
466 CoV-2 Testing Resources. *Am. J. Clin. Pathol.* **153**, 715–718 (2020).
- 467 8. Torres, I., Albert, E. & Navarro, D. Pooling of nasopharyngeal swab specimens  
468 for SARS-CoV-2 detection by RT-PCR. *Journal of Medical Virology* **92**, 2306–  
469 2307 (2020).
- 470 9. Sinnott-Armstrong, N., Klein, D. & Hickey, B. Evaluation of Group Testing for  
471 SARS-CoV-2 RNA. *medRxiv* 2020.03.27.20043968 (2020).

- 472           doi:10.1101/2020.03.27.20043968
- 473   10.   Shental, N. *et al.* Efficient high-throughput SARS-CoV-2 testing to detect  
474           asymptomatic carriers. *Sci. Adv.* **6**, 5961–5972 (2020).
- 475   11.   Ghosh, S. *et al.* A Compressed Sensing Approach to Group-testing for COVID-  
476           19 Detection. *arXiv* (2020).
- 477   12.   Gan, Y. *et al.* Sample Pooling as a Strategy of SARS-COV-2 Nucleic Acid  
478           Screening Increases the False-negative Rate. *medRxiv* 2020.05.18.20106138  
479           (2020). doi:10.1101/2020.05.18.20106138
- 480   13.   Dahdouh, E., Lázaro-Perona, F., Romero-Gómez, M. P., Mingorance, J. &  
481           García-Rodríguez, J. Ct values from SARS-CoV-2 diagnostic PCR assays  
482           should not be used as direct estimates of viral load. *Journal of Infection* (2020).  
483           doi:10.1016/j.jinf.2020.10.017
- 484   14.   Buchan, B. W. *et al.* Distribution of SARS-CoV-2 PCR cycle threshold values  
485           provide practical insight into overall and target-Specific sensitivity among  
486           symptomatic patients. *Am. J. Clin. Pathol.* (2020). doi:10.1093/AJCP/AQAA133
- 487   15.   Corman, V. M. *et al.* Detection of 2019 novel coronavirus (2019-nCoV) by real-  
488           time RT-PCR. *Eurosurveillance* **25**, 2000045 (2020).
- 489   16.   Hay, J. A., Kennedy-Shaffer, L., Kanjilal, S., Lipsitch, M. & Mina, M. J.  
490           Estimating epidemiologic dynamics from single cross-sectional viral load  
491           distributions. *medRxiv* 2020.10.08.20204222 (2020).  
492           doi:10.1101/2020.10.08.20204222
- 493   17.   Cleary, B. *et al.* Using viral load and epidemic dynamics to optimize pooled  
494           testing in resource-constrained settings. *Sci. Transl. Med.* eabf1568 (2021).  
495           doi:10.1126/scitranslmed.abf1568
- 496   18.   Singanayagam, A. *et al.* Duration of infectiousness and correlation with RT-

- 497 PCR cycle threshold values in cases of COVID-19, England, January to May  
498 2020. *Eurosurveillance* (2020). doi:10.2807/1560-  
499 7917.ES.2020.25.32.2001483
- 500 19. Gorzalski, A. J. *et al.* Characteristics of viral specimens collected from  
501 asymptomatic and fatal cases of COVID-19. *J. Biomed. Res.* **34**, 431–436  
502 (2020).
- 503 20. Tom, M. R. & Mina, M. J. To Interpret the SARS-CoV-2 Test, Consider the  
504 Cycle Threshold Value. *Clin. Infect. Dis.* **71**, 2252–2254 (2020).  
505  
506

507 **Figures and figure legends**

508 **Figure 1**



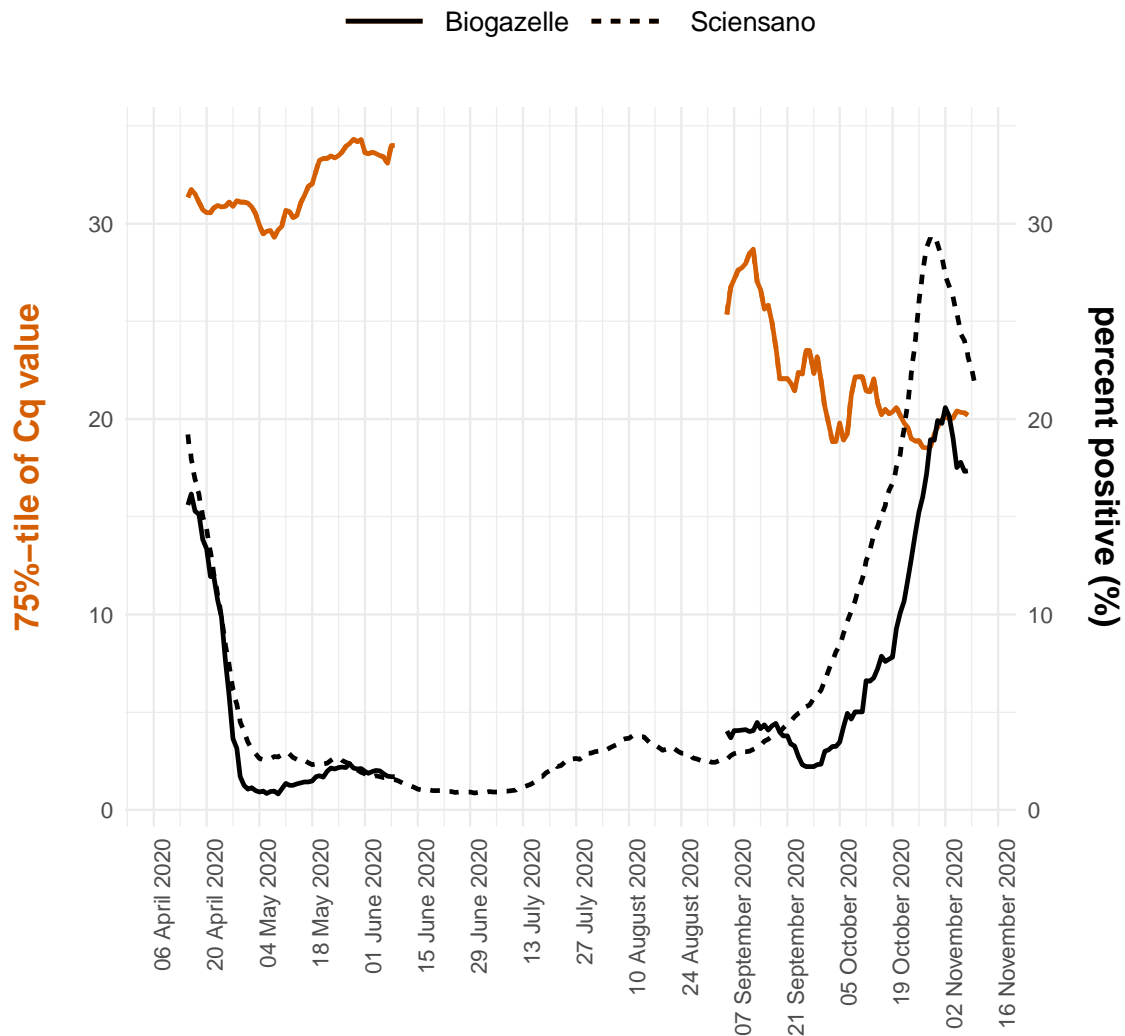
509

510 **Figure 1:** Schematic overview of the applied pooling strategies. The samples are represented as wells  
511 in a 96-well microtiter plate. The color of the wells indicates the samples' SARS-CoV-2 RNA  
512 concentration. In 1D pooling, the pools are created by row, the pools are tested and the samples in  
513 positive pools are tested again individually. During 2D pooling, the pools are created by row and  
514 column (each sample exists in two pools), the pools are tested, all negative rows and columns are  
515 removed and the remaining samples are tested individually. The sensitivity and the efficiency are  
516 calculated according to the equations found in the methods.

517



518 **Figure 2**

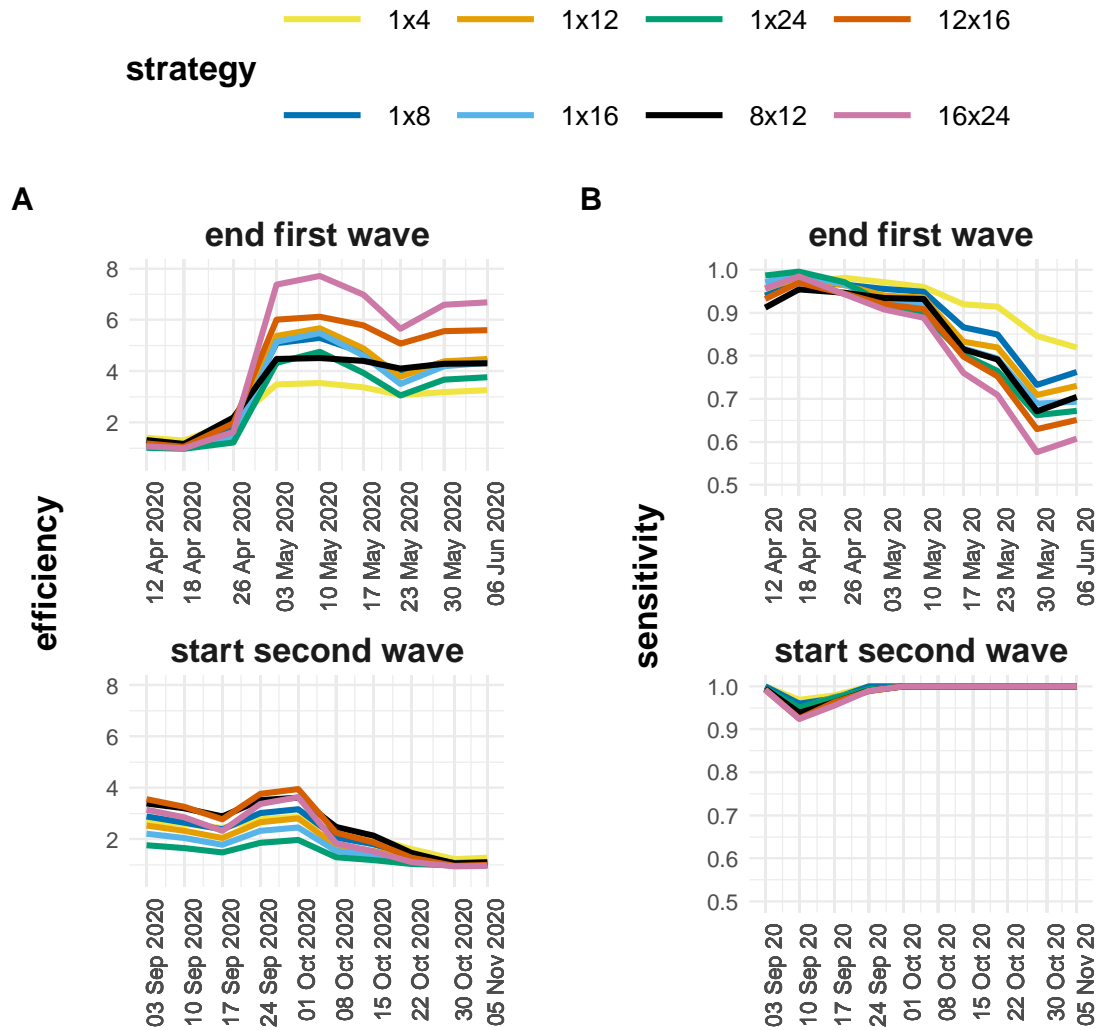


519

520 **Figure 2:** Evolution of the 75%-tile of the Cq value distribution and fraction of positive samples. The  
521 left y-axis shows the seven day moving window average of the 75%-tile of the Cq value distribution of  
522 the data originating from Biogazelle and the right y-axis shows the seven day moving window average  
523 of the fraction of positive samples for the Biogazelle and Sciensano data. The two datasets are  
524 differentiated by the line type. If the moving average was calculated using on the basis of less than  
525 five days (due to no data being available for specific days), the datapoint was removed from the  
526 visualization.

527

528 **Figure 3**



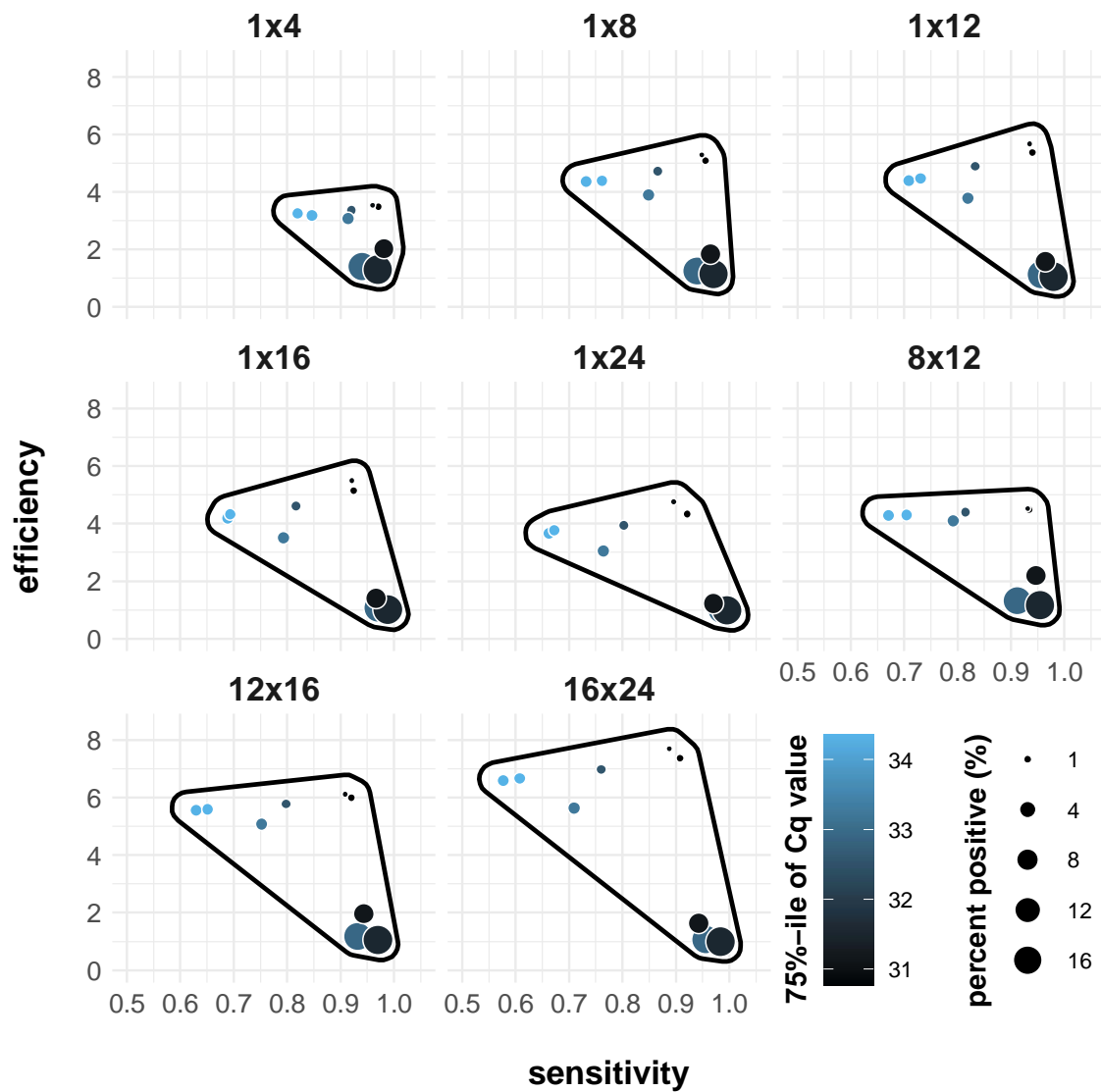
529

530 **Figure 3:** Sensitivity and efficiency for the end of the first (A) and the start of the second (B) Belgian  
531 SARS-CoV-2 infection wave. The data is grouped by week and the sensitivity and efficiency are  
532 calculated by simulating different pooling strategies (1x4, 1x8, 1x12, 1x16, 1x24, 8x12, 12x16 and  
533 16x24). The pooling strategies can be distinguished by color.

534

535 **Figure 4**

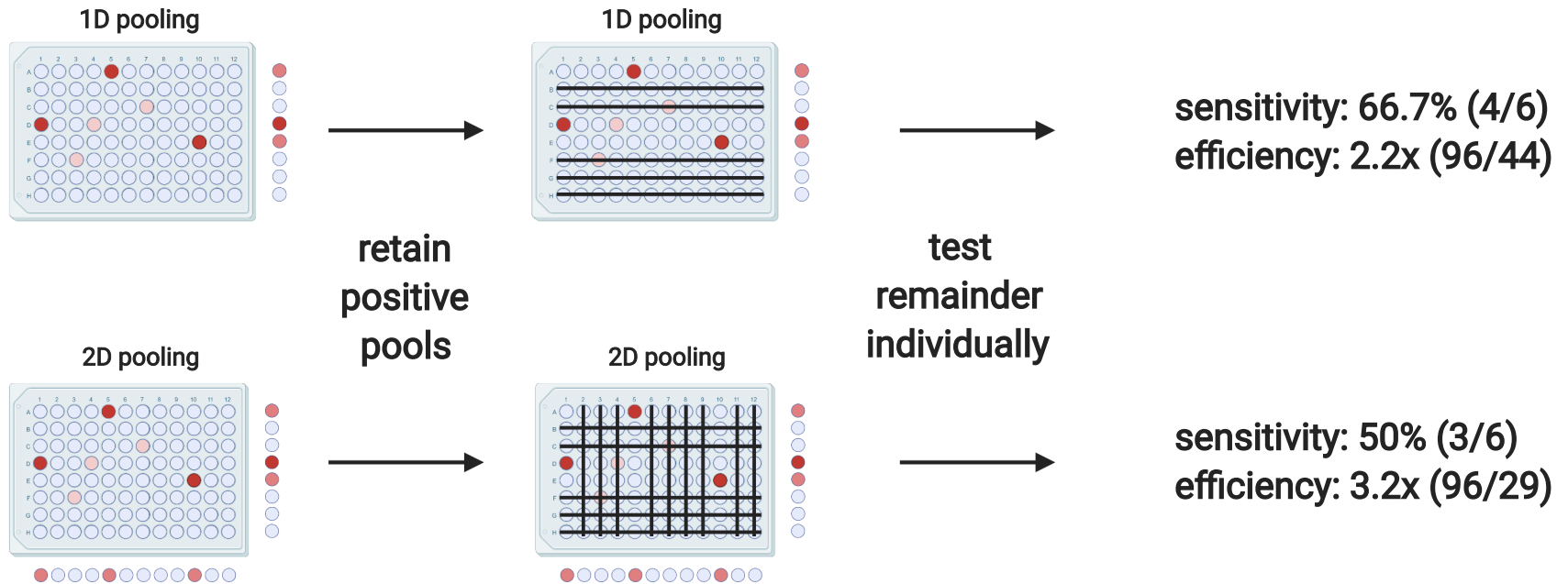
536



537

538 **Figure 4:** Simulated sensitivity and efficiency for the end of the first wave visualized with relation to  
539 the week (different circles), fraction of positive samples (size of circles) and 75%-tile of the Cq value  
540 distribution (color). A polygon is drawn around the datapoints (with a small margin) to visualize and to  
541 compare the variability of the sensitivity and efficiency over a period of time between pooling  
542 strategies.

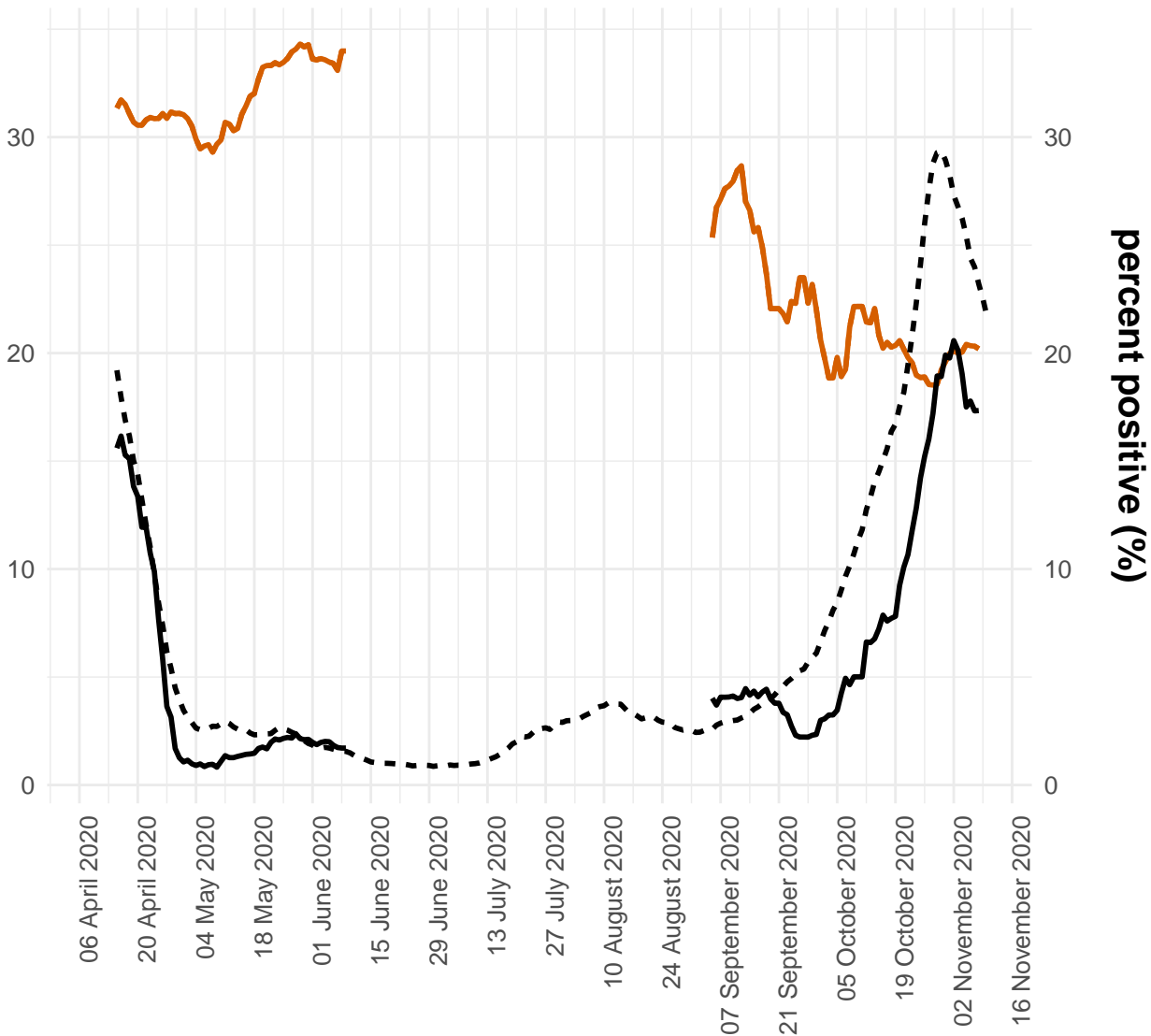
543



- negative sample
- high Cq value positive
- low Cq value positive

75%-tile of Cq value

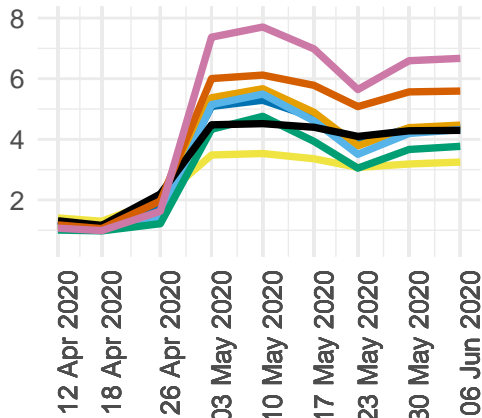
— Biogazelle - - - - - Sciensano



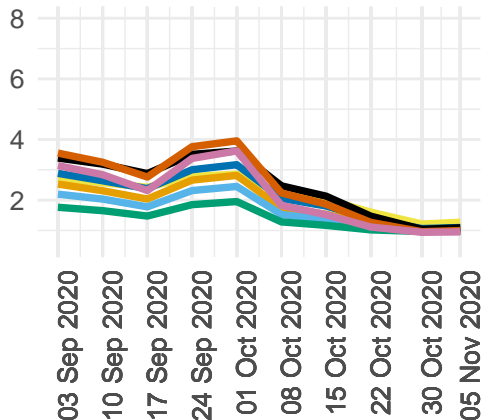


**A**

**end first wave**



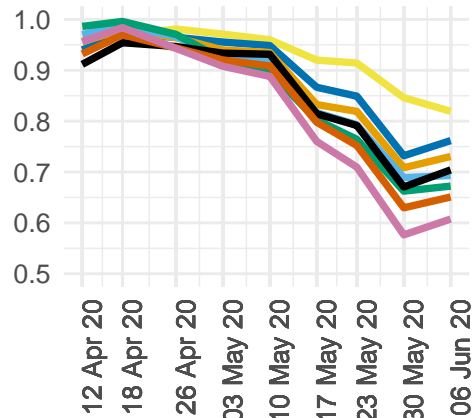
**start second wave**



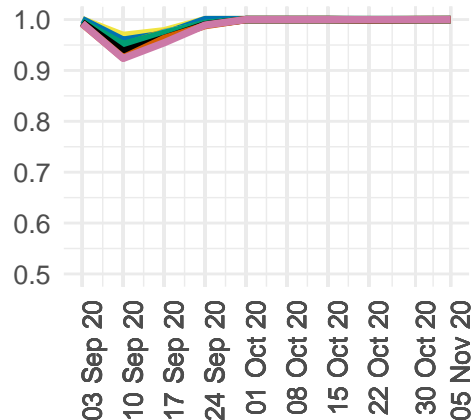
**efficiency**

**B**

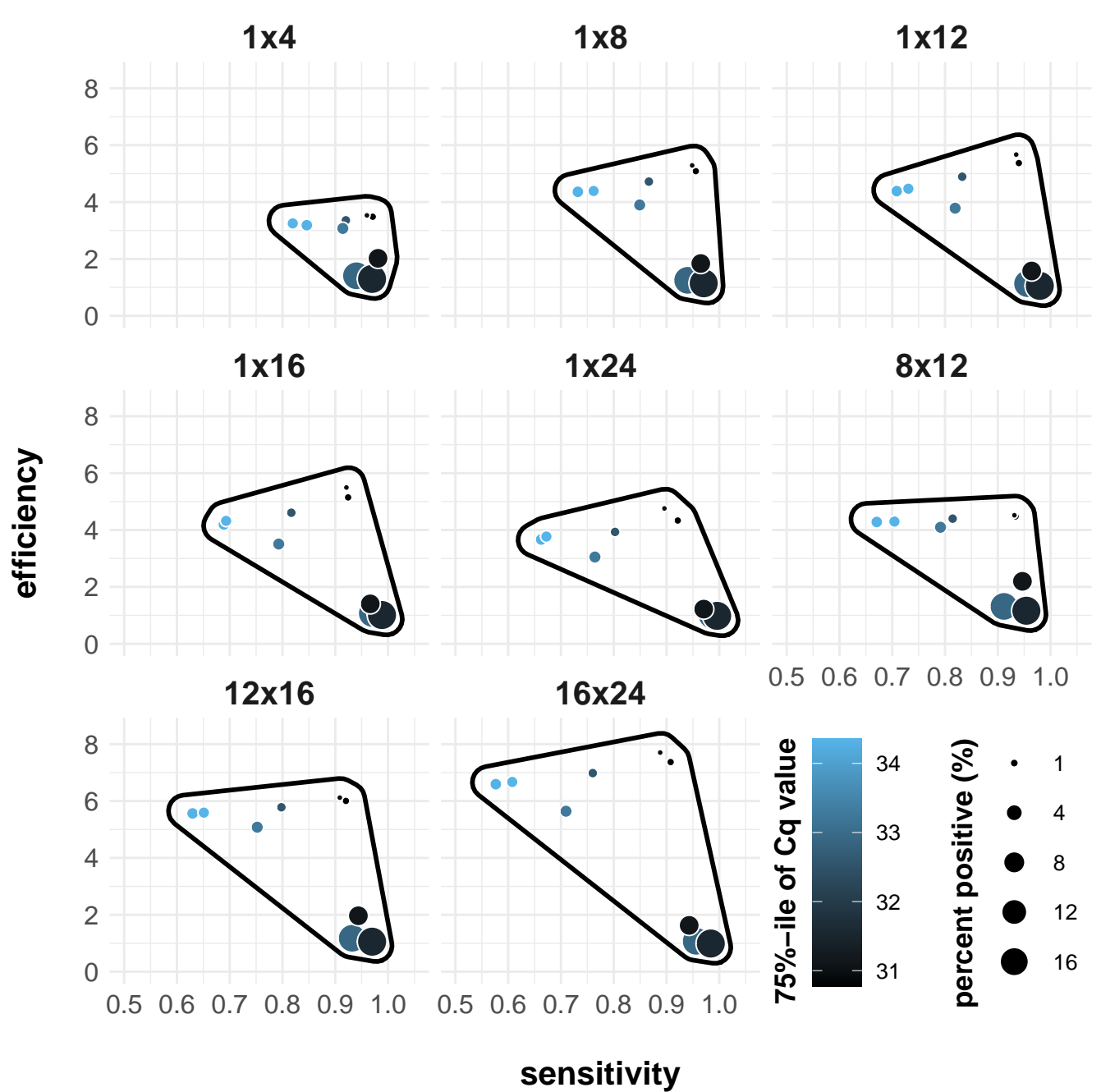
**end first wave**

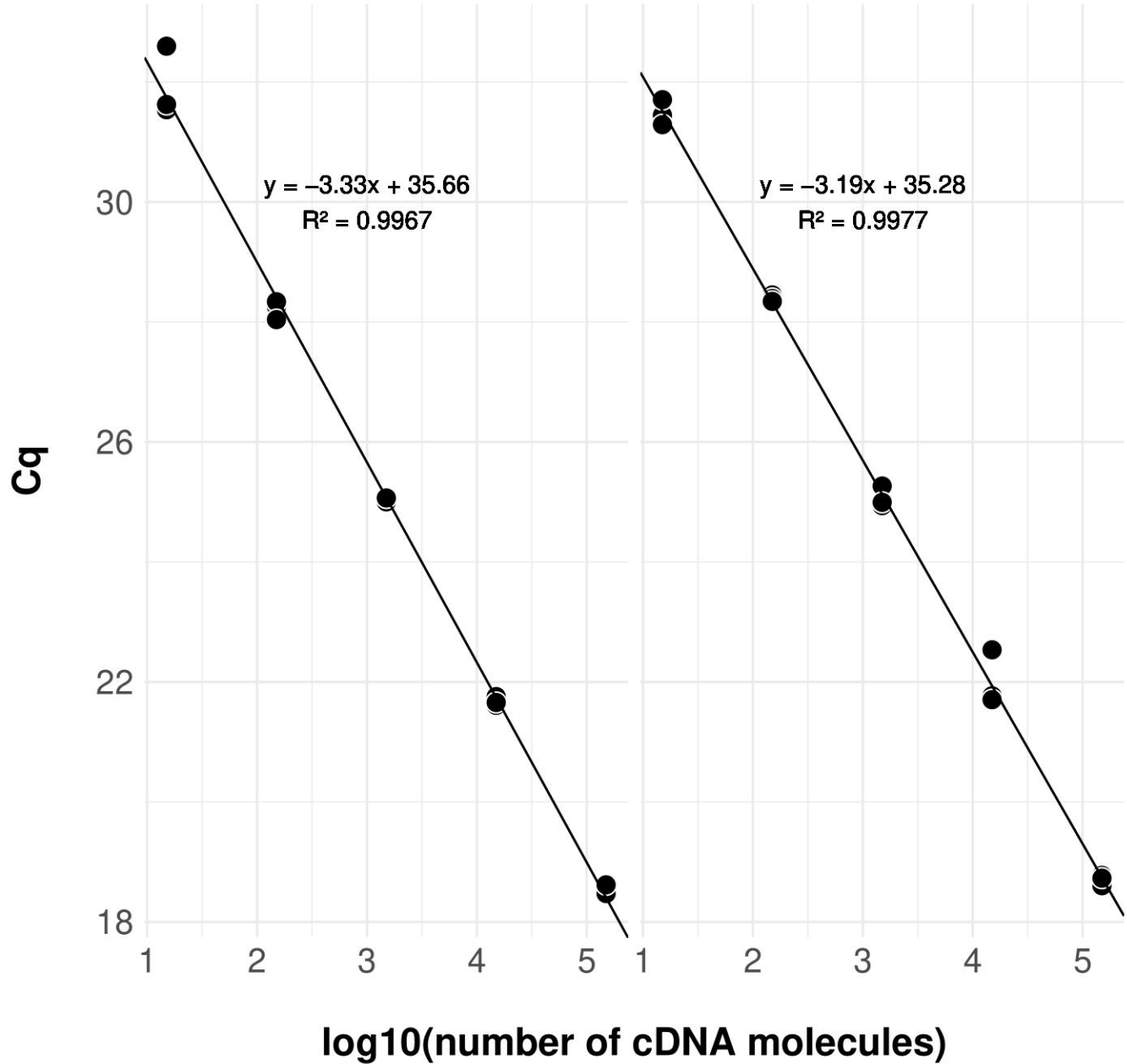


**start second wave**



**sensitivity**

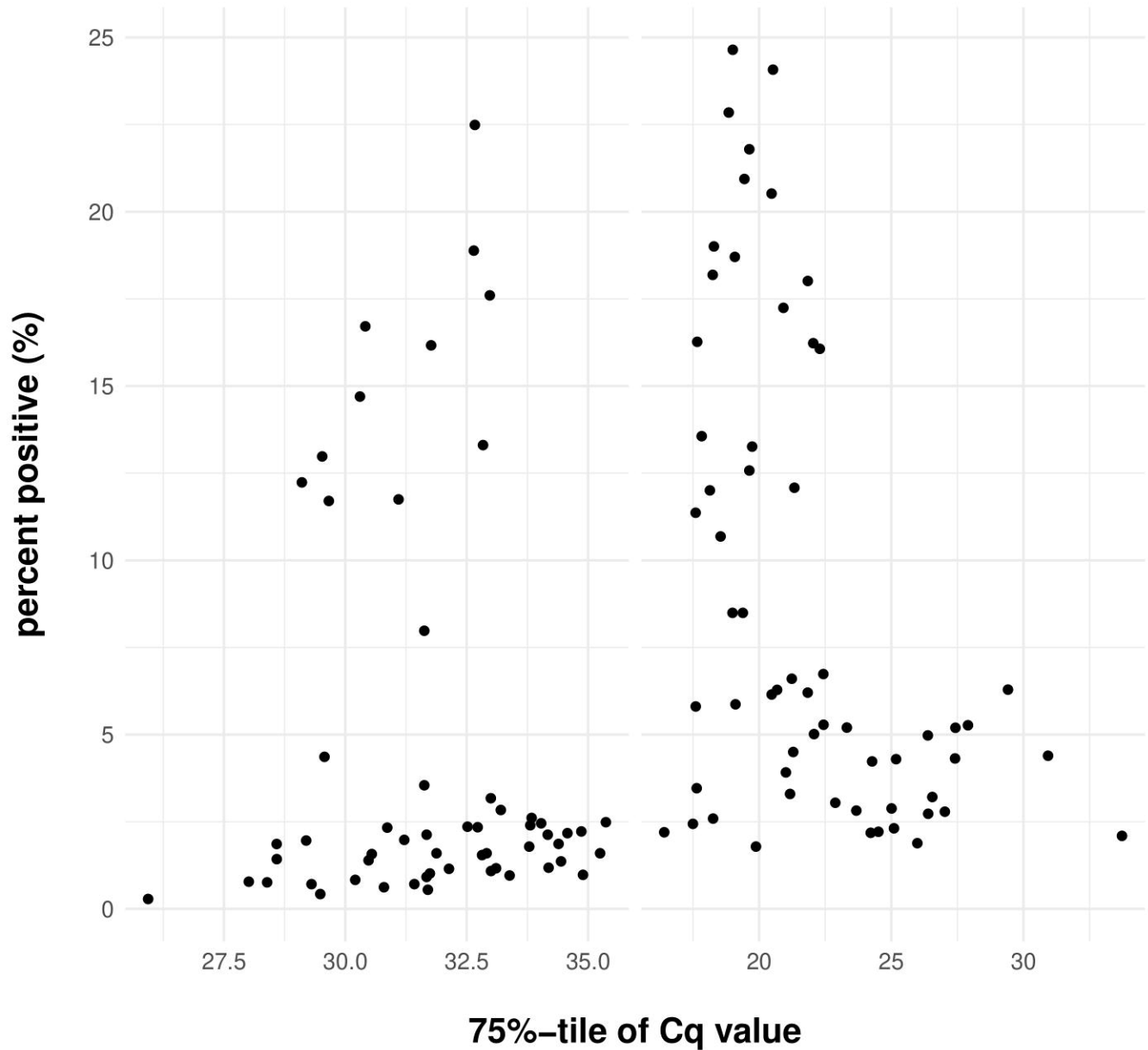


**singleplex****duplex**



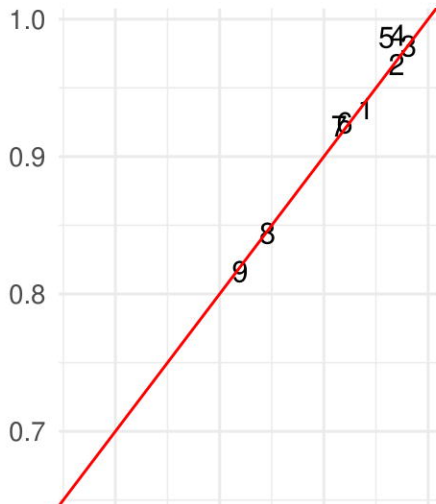
**first wave**

**second wave**

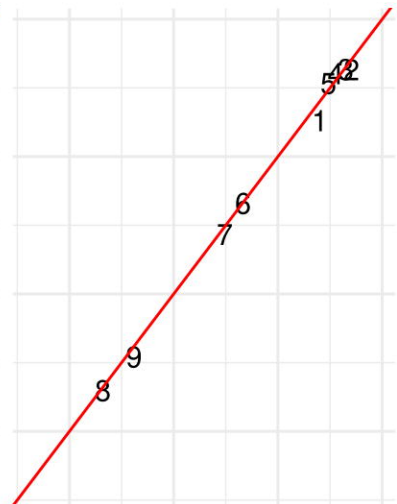


**sensitivity from calculations**

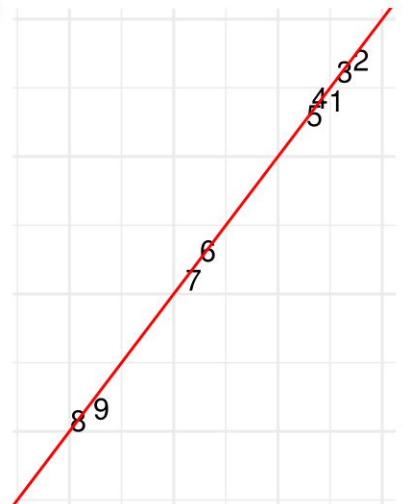
**4**



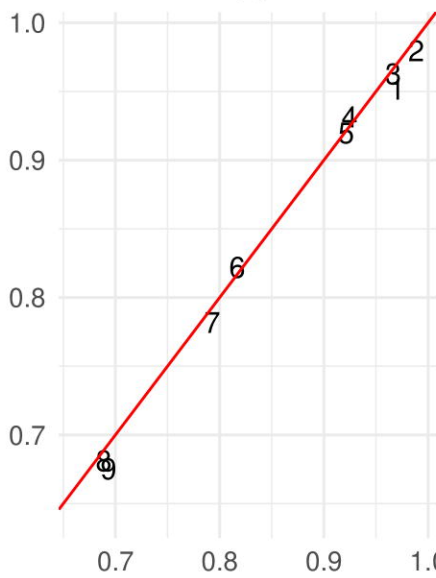
**8**



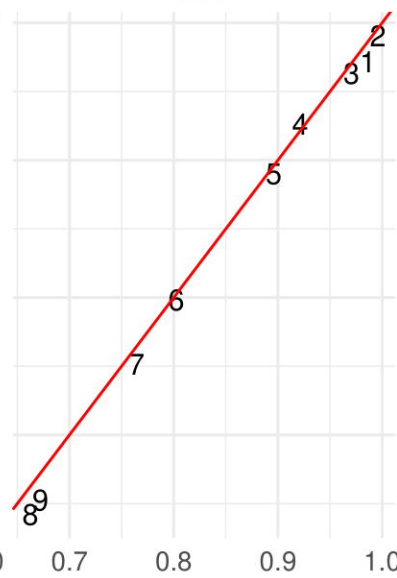
**12**



**16**



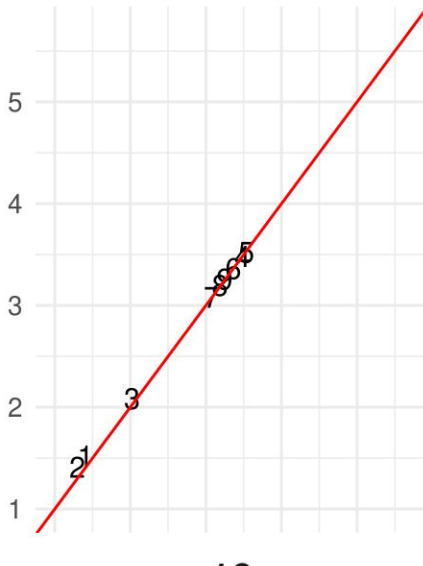
**24**



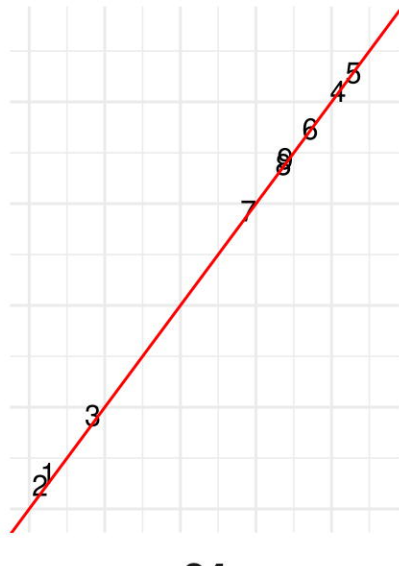
**sensitivity from simulations**

efficiency from calculations

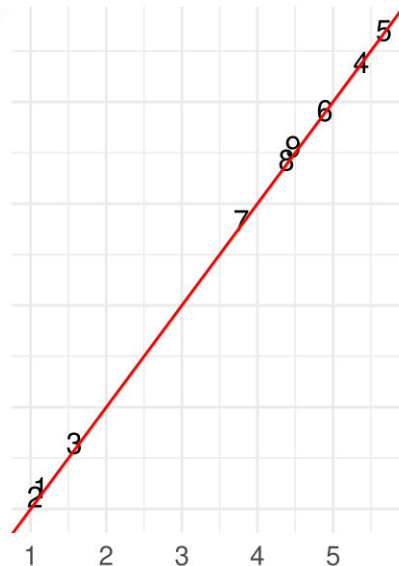
4



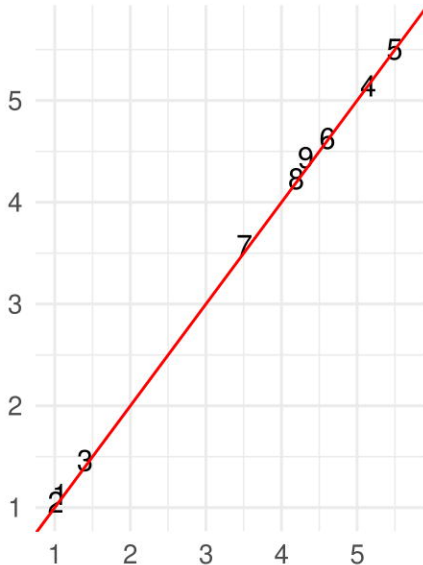
8



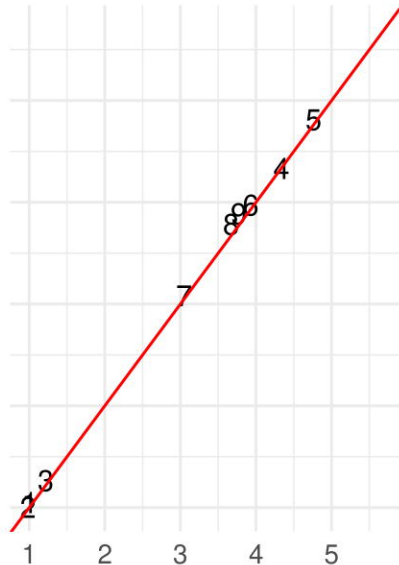
12



16



24



efficiency from simulations

Upload dataset

Browse... demo\_dataset\_Cq\_values.csv  
 Upload complete

Download demo dataset

Prevalence in %:

1

Cq threshold:

37

Pool size range:

Slider from 2 to 24

## Estimate sensitivity and efficiency of a 1D sample pooling strategy (version 1.0)

This application calculates the sensitivity and efficiency for 1D pooling strategies from custom uploaded RT-qPCR data (Cq values). The efficiency is the number of samples divided by the number of tests required. The sensitivity is the number of true positives (upon pooling and retesting individuals from positive pools) divided by the actual number of positives. This application is based on the results from "Evaluation of efficiency and sensitivity of 1D and 2D sample pooling strategies for diagnostic screening purposes" by Verwilt et al. (under review). In case you have any questions, please contact jasper.verwilt@ugent.be.

### How to use the app

1. Upload your dataset with Cq values from positive samples in .csv format. Use a point as decimal separator.
2. Fill in your estimated prevalence.
3. Fill in your single-molecule Cq value (i.e. Cq value corresponding to a single cDNA molecule; alternatively, the Cq value threshold above which you consider a sample negative).
4. Use the slider to indicate the range of pool sizes you would like to explore

You can download the demo dataset to examine what the data should look like. A new graph will automatically be generated once one of the input values changes. The efficiency is shown in black and the sensitivity is shown in green. Vertical dashed lines indicate the pool size for which the efficiency and sensitivity reach their maximal value.

